uc3m | Universidad Carlos III de Madrid

e-Archivo

This is a postprint version of the following published document:

Rubio-López, A., Olmedo, A., & Santiuste, C. (2015). Modelling impact behaviour of all-cellulose composite plates. Composite Structures, 122, 139-143.

doi:https://doi.org/10.1016/j.compstruct.2014.11.072

© Elsevier, 2014

This work is licensed under a Creative Commons Attribution-NonCommercial-NoDerivatives 4.0 International License.

Modelling impact behaviour of all-cellulose composite plates

*A. Rubio-López, A. Olmedo, C. Santiuste**

Department of Continuum Mechanic and Structural Analysis, University Carlos III of Madrid, Avda de la Universidad 30, 28911, Leganés, Madrid, Spain

*Corresponding author: Phone +34916249965, csantius@ing.uc3m.es

Abstract

All-Cellulose Composites (ACC) are entirely manufactured from cellulose, resulting a fully biodegradable material with perfect compatibility between matrix and reinforcement. In this study, a finite element numerical model to predict the low-velocity impact behaviour of ACC laminates is reported for the first time. The model was validated through comparison with experimental data from scientific literature conducted on ACC plates made from Cordenka woven plies. In addition, the model was applied to the analysis of failure modes and influence of impact energy.

Keywords: Biodegradable composites; Impact behaviour; Finite Element Analysis; All-Cellulose Composite

1. INTRODUCTION

Composite material are characterised by the combination of at least two materials, usually polymer matrix reinforced with carbon of glass fibres, with the intention to get properties that cannot be achieved using the constituent materials separately. In the last years, numerous researchers have introduced natural fibres as reinforcement to increase the biodegradability of composites. The works that have studied biocomposites made of natural fibres as jute, hemp, linen or cotton have shown promising results related with their mechanical properties [1-6]. However, the high properties of natural fibres cannot

be fully exploited in many biocomposites due to poor bonding between natural fibres and polymer matrix [7].

In recent years, a new class of monocomponent composites based on cellulosic materials, so-called all-cellulose composites (ACCs) have emerged. In ACCs, both the matrix and reinforcement are cellulosic, but the first is isotropic while the latter is highly anisotropic [8]. Nishino [9] introduced the concept of ACC materials to overcome problems associated with the compatibility and interfacial adhesion of matrix and reinforcement using chemically identical materials. In addition, the fact that such materials are fully bio-based and fully biodegradable will certainly improve their relevance in future applications [10, 11]. Huber and his collaborators published an excellent review reporting the different processing routes that have been applied to the manufacture of ACCs using a broad range of different solvent systems and raw materials [12].

The most of the research done on ACCs are focused on their behaviour under quasi-static conditions. Impact properties of ACCs are extremely important to find industrial applications e.g. in automobile structures, but these properties are difficult to quantify. Impact testing of materials is performed to determine the amount of energy that can be absorbed during a suddenly applied force. Impact testing is usually performed by Charpy or Izod test machines [6]. Charpy and Izod tests, originally designed to determine ductile–brittle transitions in metals, most often assume a pre-existing notch, which is not suitable for testing composite materials [13].

An alternative method is the drop-weight test, in which a known mass is dropped from a given height onto a flat, un-notched sample. The drop-weight test is a more realistic test of what a structural component would experience in its service life. Drop-weight tests

have proven to be valuable source of information about the impact behaviour of woven composites [14], tape laminates [15], and sandwich structures [16]. However, the use of these tests on biocomposites has not received comparable attention in scientific literature. Only a recent work published by Huber and his co-workers [17] has studied the impact behaviour of ACC plates subjected to low-velocity impact produced by a drop-weight test.

The development of theoretical models to predict the impact behaviour of composites has shown to be useful tool to get a better understanding the failure modes and the energy absorption mechanisms [15, 16, 18, 19]. However, the modelling of ACCs structures is an almost unexplored field. This work is focussed on the development of the first numerical model to predict the low-velocity impact behaviour of ACC plates using finite element method (FEM). The numerical model was validated with experimental data published in [17]. Moreover, the FEM model was used to analyse the influence of impact energy on the peak force and absorbed energy during impact. The threshold energy that produced the striker penetration was also estimated.

2. MODEL DESCRIPTION

A FEM model reproducing low-velocity impact tests on ACCs was developed using ABAQUS/Explicit code.

2.1.Material modelling

Two solids are involved in the impact test, striker and ACC plate. The striker was modelled using a linear elastic behaviour (E = 210 GPa, υ = 0.3). The ACC plate was modelled using a modification of the Hashin failure criteria [20] implemented in a VUMAT user subroutine. The model was modified because Hashin criteria was developed for tape plies, while the ACC plates analysed in this work were manufactured

from woven plies. These modifications for woven laminates were similar to those developed by Lopez-Puente et al. to modify Hou criteria for tape laminates [21].

Fibre failure. This damage criterion considers tensile and compressive fibre breakage in directions 1 and 2. Thus two different equations were used, Eq. (1) for fibres at 0º and Eq. (2) for fibres at 90º:

$$d_{f1} = \left(\frac{\sigma_{11}}{X_T}\right)^2 + \left(\frac{\tau_{12}}{S_f}\right)^2 \qquad (1)$$

$$d_{f2} = \left(\frac{\sigma_{22}}{Y_T}\right)^2 + \left(\frac{\tau_{12}}{S_f}\right)^2 \qquad (2)$$

Where X_T and T_Y are tensile strength in 1 and 2 directions respectively, and they have the same value for this material; S_f is the shear strength; σ_{11} and σ_{22} are the normal stress in directions 1 and 2; and τ_{12} the shear stress. When one of these damage variables equals one, all the stress components are set to zero.

Matrix failure was predicted using the next equation:

$$d_d = \left(\frac{\sigma_{33}}{Z_r}\right)^2 + \left(\frac{\tau_{13}}{S_f}\right)^2 + \left(\frac{\tau_{23}}{S_f}\right)^2 \qquad (3)$$

Where Z_r is the interlaminar strength; and τ_{13} and τ_{23} are the corresponding out-of plane shear stresses. Eq. (3) is applied only to out-of-plane tensile stresses ($\sigma_{33} > 0$). When this damage variable equals one, all the stress components that appear in the equation are set to zero.

To avoid sudden changes in the stiffness of the finite elements when damage occurs leading to instability problems and lack of convergence during the simulation, the stress components were corrected using a smooth transition, Eq. (4).

$$\sigma_{ij}^{cor} = \sigma_{ij} \cdot \left(1 - \frac{2 - e^{s(d_i - 1/2)}}{2 - e^{s/2}}\right) \qquad (4)$$

Where σ_{ij} and σ^{cor}_{ij} are the stress before and after the correction, d_i is the corresponding damage parameter, and s is the variable that controls the slope of the stress decay when the damage is close to 1. The value s = 30 was adopted according to [21].

Moreover, the simulation of the impact involves the perforation of the plate, thus a finite element erosion criterion is required. When damage occurs in an element, the stresses on it drop to zero and large deformations appear. A maximum strain criterion was adopted to remove the distorted elements: after each time increment the longitudinal strains (ε_1, ε_2 and ε_3) are calculated; if one of them reaches a critical value ($\varepsilon_i = 1$) the element is removed. Thus, erosion criterion only affects to elements that have been already degraded.

It should be noticed that this model is based on the assumption of the hypothesis of linear-elastic behaviour up to failure. Moreover, the mechanical behaviour of ACCs is considered strain rate independent. These hypotheses have been widely used in the modelling of carbon and glass fibre composite [15, 16, 18, 19]. However, more experimental works and impact tests are required to prove these hypotheses in biodegradable composite. Since this is the first attempt to model the impact behaviour of ACCs, these assumptions are provisionally considered to explore the model accuracy to reproduce the behaviour of ACC plates.

2.2.Geometry and boundary conditions

The geometry of the model reproduced the experimental tests reported in [17]. The plate consisted on a circular plate of diameter (D_p) 40mm and thickness (t_p) 2mm composed

of five Cordenka layers. The striker was modelled as a hemispherical solid of diameter (D_s) 20mm with a mass of 9.54kg, as shown in Fig. 1.

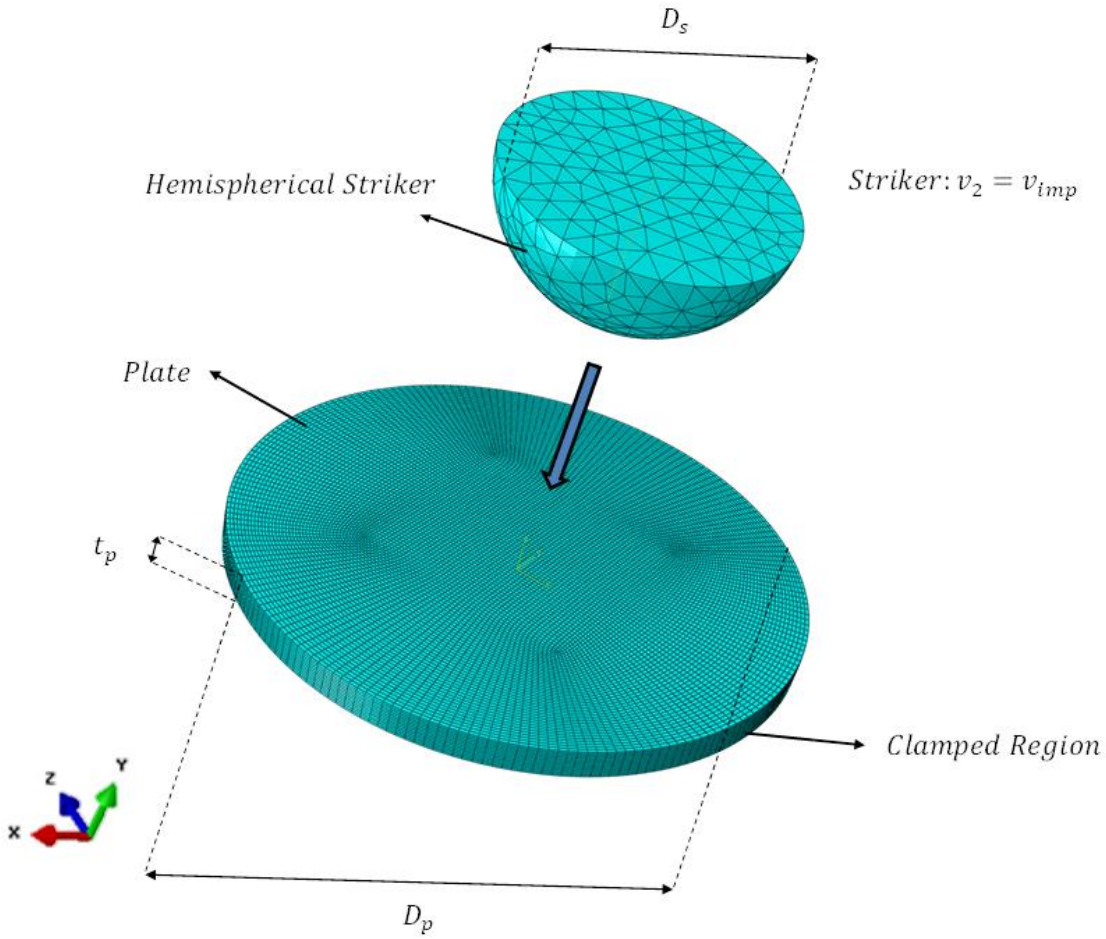

Fig.1. Finite element model. Geometry and boundary conditions.

The ACC plate was made of Cordenka fibres using ionic liquid BimimAc as solvent. The mechanical properties of Cordenka ACC plates were reported by Huber´s research group in [17] and [22]. The density, elastic modulus, and tensile strength are 450 g/m^2, 3.72 GPa, and 91.2 MPa respectively. The shear strength (S_f) was set in 52.65 Mpa using Eq. (5) proposed by Bledzki [6].

$$S_{12} = \frac{X_T}{\sqrt{3}} \qquad (5)$$

The external surface of the plate was clamped to reproduce the experimental tests boundary conditions. An initial velocity of 4.17m/s (v_{imp}) was imposed to the striker leading to impact energy of 83.71 J. Fig. 1 shows the geometry and boundary condition.

Moreover, an interaction contact was defined between the striker surface and a node region that included all the plies of the plate. The interaction contact was modelled using the algorithm surface-node surface contact available in ABAQUS/Explicit.

2.3.Finite element mesh

The sensitivity of the mesh was analysed with successive space discretization. The selected mesh for the plate had 134784 linear brick elements, with reduced integration (C3D8R). The striker was modelled with 5890 quadratic tetrahedral elements (C3D10M). The three dimensional non-homogeneous mesh, with smaller elements in the contact area is shown in Fig. 1.

3. RESULTS AND DISCUSSION

3.1. Model validation.

To validate the FEM model the numerical results were compared with the experimental data from [17] in terms of force-displacement curve and absorbed energy. Fig. 2 shows the comparison between experimental and numerical force-displacement curves. An excellent agreement between numerical prediction and experimental data was found. The model showed an accurate prediction of stiffness, peak force and force drop after damage. The numerical and experimental peak forces were 3.87kN and 3.68kN respectively, with an error of 5.16%.

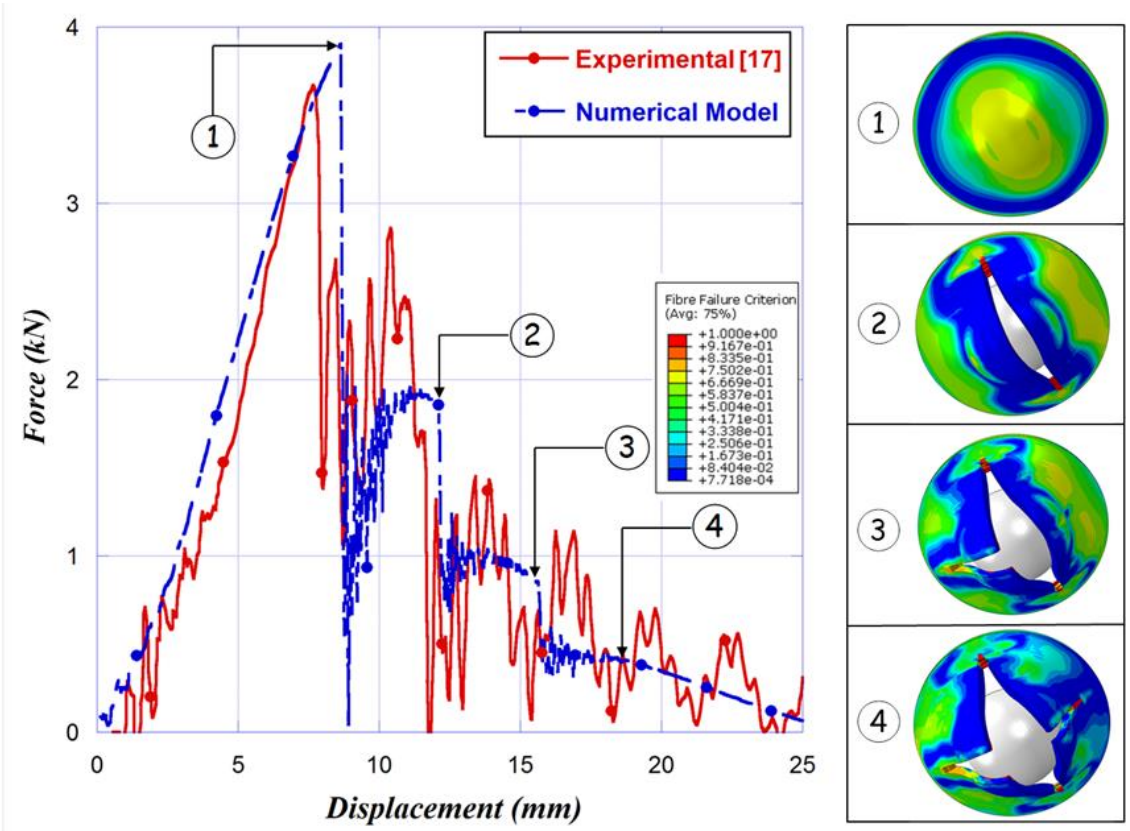

Fig.2. Force-displacement curve (numerical and experimental results) and damage evolution.

The force displacement curves were integrated to calculate the energy absorbed by the ACC plate during the impact process. The evolution of the absorbed energy is shown in Fig. 3. The numerical model overestimated the absorbed energy but the evolution of the numerical predictions agreed with the experimental results. The total absorbed energy according to numerical and experimental results are 28.27 J and 26.04 J respectively, resulting in an error of 8.56%.

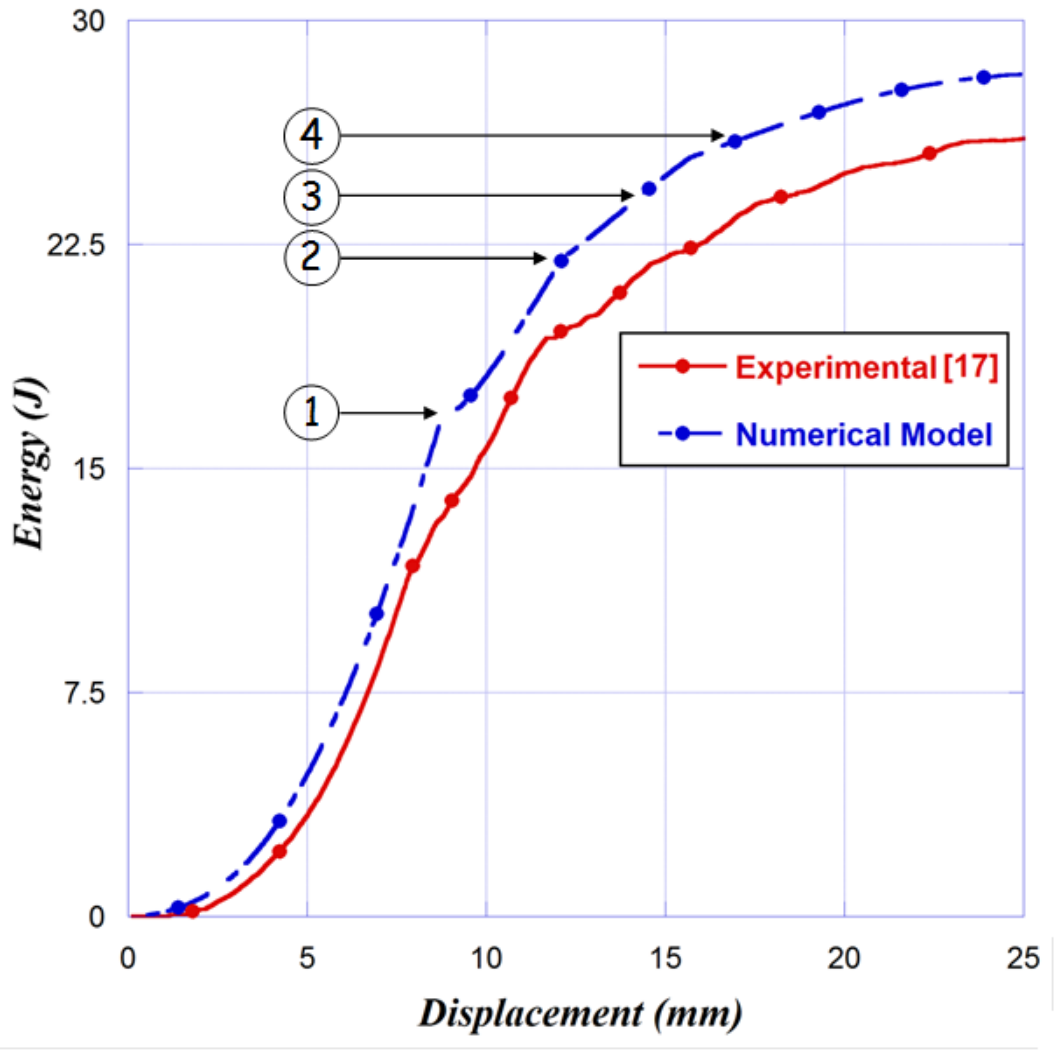

Fig.3. Absorbed energy versus striker displacement. Comparison between numerical and experimental results.

3.2. Damage mechanisms.

FE model results were used to analyse the damage mechanisms that produced the failure of the ACC plate. The deformed shape of the plate at some relevant points of the force-displacement curve is shown in Fig. 2. The main failure criterion according to the simulations was fibre breakage in agreement with the results reported in [17], thus Fig. 2 represents the field of the fibre failure criterion.

The first point corresponds to the previous moment to the force drop, the failure criterion is lower than one in all the elements thus no damage was found in the plate. The second point, after the first force drop, shows the first crack propagation produced by fibre failure due to tensile stresses. The third point, after the second force drop, shows a second crack in perpendicular direction. Finally, the fourth point corresponds to a point after the third force drop. At this point, a new crack appears leading to the pyramidal shape failure observed in the experimental tests [17]. These results show that the progressive failure of the ACC plate is a consequence of the consecutive cracks that are propagated during striker penetration. The FEM model was able to reproduce force history and damage mode observed in experimental tests.

3.3. Influence of impact energy

In addition, the validated FEM model was applied to analyse the influence of impact energy. The initial impact velocity of the striker was modified to study the behaviour of the ACC plate under impact energies from 0 to 83.71 J. Fig.4 shows the evolution of peak force and absorbed energy with the impact energy. Three stages can be observed in this curve.

The first stage correspond to impact energy from 0 to 1.2 J. The behaviour of the plate was elastic thus the absorbed energy was zero. The peak force increased linear with impact energy. No damage was observed in the plates.

In the second stage, for impact energy from 2 J to 30 J, the value of the absorbed energy increased with increasing impact energies. In these impacts the plate was damaged but not penetrated by striker. On the other hand, the value of the peak force increased for impact energy from 2 J to 19 J. A crack was observed in the ACC plate for impact energies higher than 19 J, see Fig. 5b, thus the peak force was stabilised at a value

around 3800 N. The residual velocity of the striker for impact energy equal to 30 J was zero, thus 30 J was estimated as the impact energy perforation threshold.

In the third stage, impact energies higher than 30 J, the plate was perforated, Figs. 5c-d. The absorbed energy was almost constant because the impact energy was higher than the energy absorbing capability of the ACC plate. Failure mode observed corresponded to fibre breakage and subsequent crack propagation in principal directions leading to a four-petal pyramid shape.

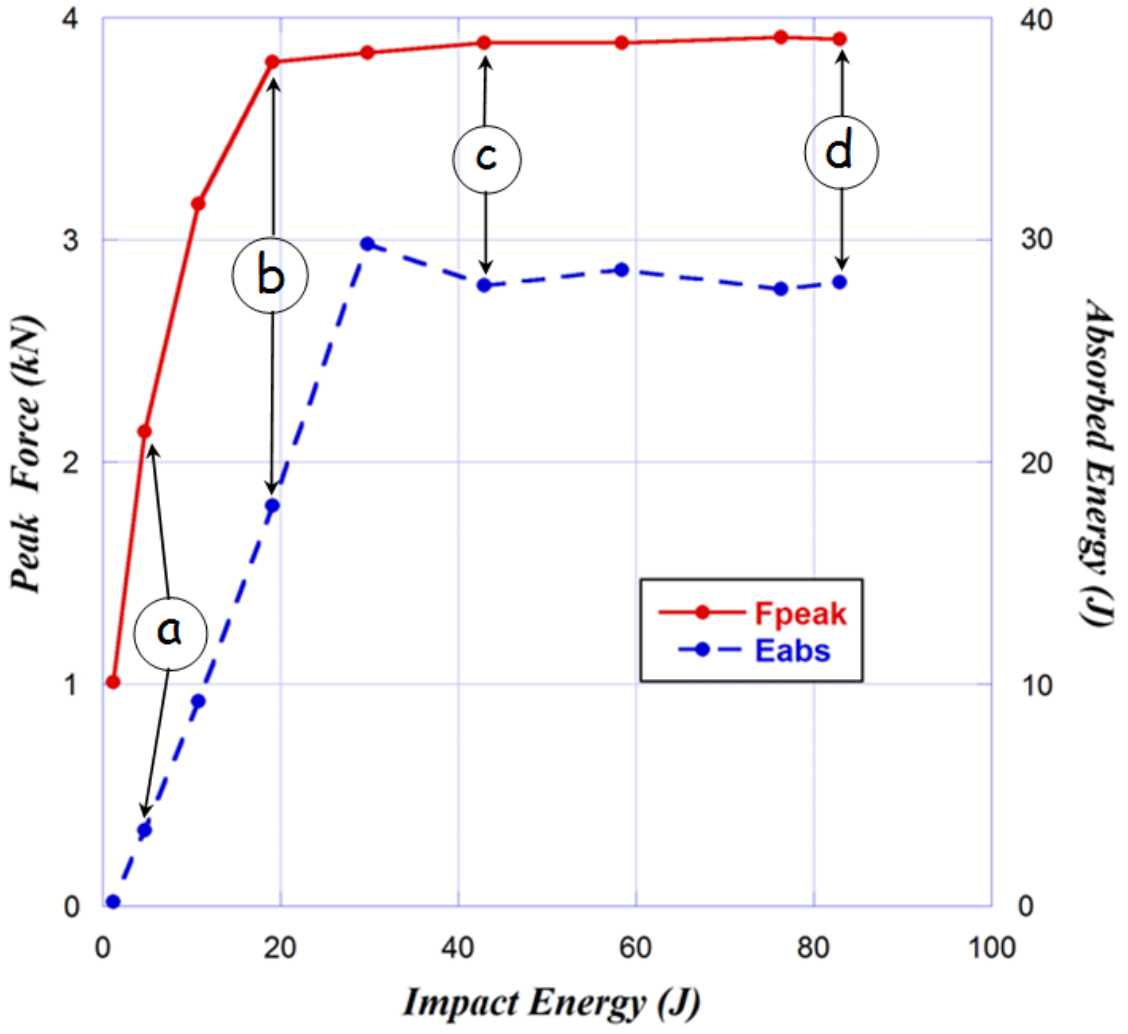

Fig.4. Peak force and absorbed energy versus impact energy. Numerical results.

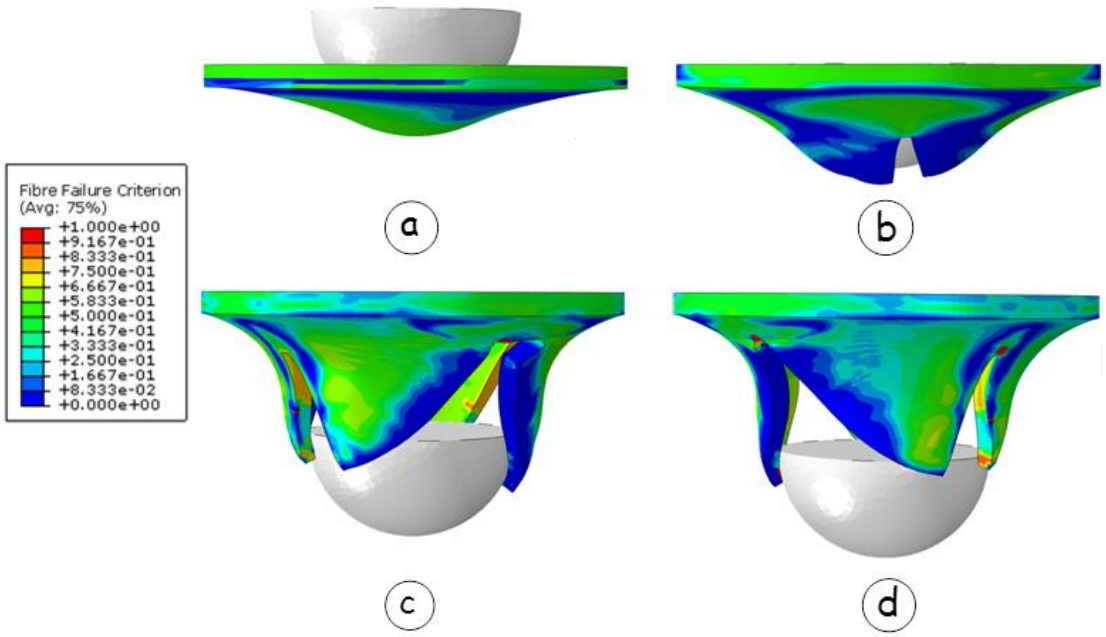

Fig.5. Failure modes under different impact energies. A) impact energy 4.77 J. b) impact energy 19.08 J: . c) impact energy 42.93 J. d) impact energy 83.71 J

4. CONCLUSIONS

A finite element numerical model to predict the behaviour of ACC plates under low-velocity impacts was presented for the first time. The model was validated through comparison with experimental results. Force-displacement curve, absorbed energy and failure modes predicted by the model were in agreement with experimental data. The results showed that the progressive failure of the ACC plate is a consequence of the consecutive cracks that appear during the striker penetration. The main failure mode was fibre breakage due to tensile stresses. Moreover, the influence of impact energy was analysed finding the impact energy threshold that produce the striker penetration.

The model presented in this work is the first step in the development of numerical models to predict the impact behaviour of biodegradable composite plates. Some of the model hypotheses, such as linear-elastic behaviour up to failure and strain-rate independence, should be analysed in future works. The promising results obtained with

this model can be useful in the development of predictive tools to provide new application for biodegradable composite materials.

REFERENCES

1. Faruk O, Bledzki AK, Fink HP, Sain M. Biocomposites reinforced with natural fibers: 2000–2010. Progress in Polymer Science 2012;37(11):1552– 1596.

2. Akil HM, Omar MF, Mazuki AAM, Safiee S, Ishak ZAM, Abu Bakar A. Kenaf fiber reinforced composites: A review. Mater Des 2011;32(8-9):4107–4121.

3. Koronis G, Silva A, Fontul M. Green composites: A review of adequate materials for automotive applications. Compos Part B: Eng 2013;44(1):120–127.

4. Tawakkal ISMA, Talib RA, Abdan K, Ling CN. Mechanical and physical properties of Kenaf-derived Cellulose (KDC)-filled polylactic acid (PLA) composites. Bioresources 2012;7(2):1643-4655.

5. Xiao-Yun W, Qiu-Hong W, Gu H. Research on Mechanical Behaviors of the Flax/Polyactic Acid Composites . Journal of Reinforced Plastics and Composites 2010;29(17):2561-2567.

6. Bledzki AK, Jaszkiewicz A. Mechanical performance of biocomposites based on PLA and PHBV reinforced with natural fibres – A comparative study to PP. Compos Sci Technol 2010;70(12):1687-1696.

7. George J, Sreekala MS, Thomas S. A review on interface modification and characterization of natural fiber reinforced plastic composites. Polym Eng Sci. 2001;41(9):1471–85.

8. Gindl-Altmutter W, Keckes J, Plackner J, Liebner F, Englund K, Laborie MP. All-cellulose composites prepared from flax and lyocell fibres compared to epoxy–matrix composites. Compos Sci Technol 2012(11);72:1304–1309.

9. Nishino T, Arimoto N. All-Cellulose Composite Prepared by Selective Dissolving of Fiber Surface. Biomacromolecules 2007;8(9):2712-2716.

10. Song YS, Lee JT, Ji DS, Kim MW, Lee SH, Youn JR. Viscoelastic and thermal behavior of woven hemp fiber reinforced poly(lactic acid) Composites. Compos Part B: Eng 2012;43:856–860.

11. Soykeabkaew N, Arimoto N, Nishino T, Peijs T. All-cellulose composites by surface selective dissolution of aligned ligno-cellulosic fibres. Compos Sci Technol 2008;68(10-11):2201–2207.

12. Huber T, Müssig J, Curnow O, Pang S, Bickerton S, Staiger MP. A critical review of all-cellulose composites. J Mater Sci 2012;47(3):1171–1186.

13. Ku H, Cheng YM, Snook C, Baddeley D. Drop weight impact test fracture of vinyl ester composites: micrographs of pilot study. J Compos Mater 2005;39(18):1607-1620.

14. Santiuste C, Sanchez-Saez S, Barbero E. Residual flexural strength after low-velocity impact in glass/polyester composite beams. Compos Struct 2010;92(1):25-30.

15. Santiuste C, Sanchez-Saez S, Barbero E. A comparison of progressive-failure criteria in the prediction of the dynamic bending failure of composite laminated beams. Compos Struct 2010;92(10):2406-2414.

16. Ivañez I, Santiuste C, Sanchez-Saez S. FEM analysis of dynamic flexural behavior of composite sandwich beams with foam core. Compos Struct 2010;92(9):2285-2291.

17. Huber T, Bickerton S, Müssig J, Pang S, Staiger MP. Flexural and impact properties of all-cellulose composite laminates. Compos Sci Technol 2013;88:92–98.

18. Buitrago BL, Santiuste C, Sánchez-Sáez S, Barbero E, Navarro C. Modelling of composite sandwich structures with honeycomb core subjected to high-velocity impact. Compos Struct 2010;92(9):2090-2096.

19. Santiuste C, Díaz-Álvarez J, Soldani X, Miguélez H. Modelling thermal effects in machining of carbon fiber reinforced polymer composites. Journal of Reinforced Plastics and Composites 2014;33(8):758-766.

20. Hashin Z. Failure criteria for unidirectional fiber composites. Trans ASME J Appl Mech 1980;47(2):329–34.

21. Lopez-Puente J, Zaera R, Navarro C. An analytical model for high velocity impacts on CFRPS woven laminates. Int Solids Struct 2007;44:2837-57.

22. Huber T, Bickerton S, Müssig J, Pang S, Staiger MP. Solvent infusion processing of all-cellulose composite materials. Carbohyd Polym 2012;90(1):730–733.